Study of Thermally Treated Lithium Montmorillonite by Ab Initio Methods

Stephen Stackhouse* and Peter V. Coveney†

Centre for Computational Science, Department of Chemistry, Queen Mary, University of London, Mile End Road, London, E1 4NS, United Kingdom

Received: April 2, 2002; In Final Form: October 10, 2002

The Hofmann−Klemen effect describes the observed reduction in expandable character and cation exchange capacity of lithium-saturated montmorillonite upon mild heating. Although it is widely accepted that the observed changes are due to the lithium ions becoming fixated within the layer structure of the clay mineral, some uncertainty still exists as to the precise location of the migrated lithium ions within the clay framework. It has been suggested that the cations reside in the ditrigonal cavities of the tetrahedral layer, the vacant octahedral sites, or both. We employ density functional methods to examine the phenomenon at the electronic structure level. We find that it is energetically preferable for lithium cations to reside in the vacant octahedral sites as opposed to the ditrigonal cavities due to the closer proximity to the negative charge sites in the octahedral layer increasing favorable Coulombic interactions. Occupation of octahedral sites causes structural hydroxyl groups to reorientate perpendicular to the *ab* plane. Deprotonation and dehydroxylation are not observed during molecular dynamics at experimentally reported temperatures. Dehydroxylation inhibits rather than facilitates cation migration. A comparison of calculated power spectra with experimental infrared spectra suggests that lithium cations do not migrate to ditrigonal cavities when no tetrahedral aluminum is present.

1. Introduction

Montmorillonite is a 2:1 layer type aluminosilicate belonging to the group of clay minerals known as smectites. It comprises an octahedral alumina layer fused between two tetrahedral silica layers. Partial substitution of octahedral aluminum by magnesium or iron and tetrahedral silicon by aluminum creates a negative structural charge, which is balanced by metal ions adsorbed into the space between layers, known as the interlayer. Hydration of the cations means that it is normal for a certain amount of water to also be accommodated within the interlayer; as relative humidity rises, the quantity of water adsorbed increases and the interlayer expands in order to accommodate the greater molecular volume between the layers.[1,2] This is known as clay swelling.

The swelling behavior of clay minerals has been studied extensively by experiment[1,2] and simulation,[3−11] and its dependence on interlayer cation species and degree and type of isomorphic substitution is now generally well-understood. However, one related phenomenon that still attracts attention is the Hofmann−Klemen effect, which describes the observed reduction in expandable character and cation exchange capacity (CEC) of lithium-saturated montmorillonite upon mild heating (200−300 °C).[12] This is the subject of the present article.

It is widely accepted that the observed changes in swelling properties and CEC are due to the lithium ions becoming fixated within the layer structure of the clay mineral—movement of the cations into the clay lattice decreases the number accessible for hydration and exchange, reducing the enthalpic driving force for the adsorption of water and subsequent swelling. However, some uncertainty still exists over the precise location of the lithium ions within the clay framework. It has been suggested that the cations migrate from the interlayer (Figure 1a) into the ditrigonal cavities of the tetrahedral layer (Figure 1b),[13−15] the vacant octahedral sites (Figure 1c),[16−18] or both of these.[19−24]

Tettenhorst was one of the first to argue that migration of cations occurs from the interlayer into the ditrigonal cavities of the tetrahedral layer without deeper penetration into unfilled octahedral sites, based on a lack of association of the metal ions with apical oxygens, inferred from infrared spectroscopy.[13] More recent evidence for the location of the cations exclusively in the ditrigonal cavities exists in the form of two complementary magic angle spinning nuclear magnetic resonance (MAS NMR) studies. ^{27}Al MAS NMR carried out by Alvero et al. showed distortion of the tetrahedra of oxygen atoms surrounding aluminum in the tetrahedral layer, attributed to lithium ions located in ditrigonal cavities.[14] This was supported by demonstration of the reversible migration of lithium in montmorillonite under high water vapor pressure, which tends to imply that in a collapsed mineral lithium ions are situated close to the interlayer region where the water molecules can access them. ^{7}Li MAS NMR performed by Theng et al. showed that the low symmetry chemical environment of lithium ions in heated montmorillonite is very different from those occupying octahedral sites in hectorite and lepidolite, indicating their location in distorted ditrigonal cavities.[15]

Although no authors claim that lithium ions migrate exclusively to vacant octahedral sites, some imply this by lack of any mention of cations being present in the ditrigonal cavities.[16−18] Evidence offered for the occupation of vacant octahedral sites has come almost entirely from infrared studies,[16−23] which compare the spectra of untreated and thermally treated lithium montmorillonite, particularly those bands assigned to hydroxyl stretching and bending modes, found between 3300 and 3800 cm^{-1} and 650−1000 cm^{-1}, respectively. In addition, some studies also examine Si−O vibrational modes in the 400−1300 cm^{-1} region.[18,21−23]

* To whom correspondence should be addressed. Tel: ++44(0)20 7882 7759. Fax: ++44(0)20 7882 7794. E-mail: s.stackhouse@qmul.ac.uk.
† E-mail: p.v.coveney.qmul.ac.uk.

10.1021/jp025883q CCC: $22.00
Published on Web 11/02/2002

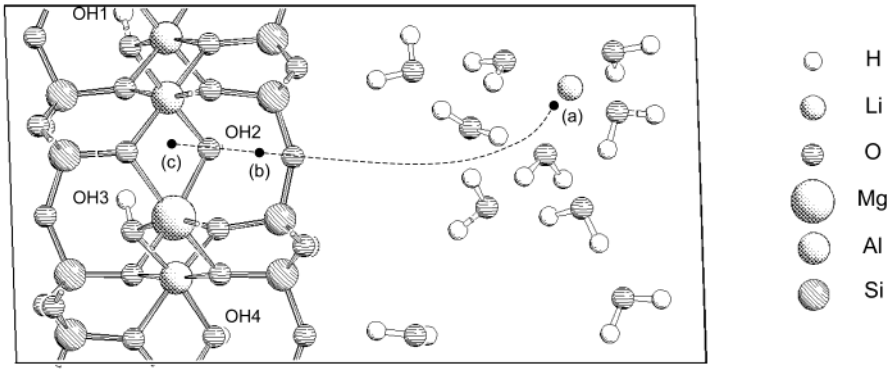

Figure 1. Lithium montmorillonite unit cell. Upon thermal treatment, the lithium cations are thought to migrate from the interlayer (a) into the ditrigonal cavities of the tetrahedral layer (b), the vacant octahedral sites (c), or both of these. Three-dimensional periodic boundary conditions are applied at the edges of the cell, as indicated by the solid lines.

One of the most important infrared studies is that by Calvet and Prost who reported the appearance of dichroic bands in the hydroxyl stretching region of the infrared spectrum of lithium montmorillonite upon heat treatment.[19] These were attributed to hydroxyl groups orientated perpendicular to the *ab* plane, since such hydroxyls do not contribute to the absorption under normal incidence. Computations based on a point charge model presented in the same paper showed that in montmorillonite structural hydroxyl groups must reorientate perpendicular to the *ab* plane upon filling of vacant octahedral sites. This led the authors to conclude that the appearance of dichroic bands was indicative of the migration of lithium cations to the octahedral layer. Many subsequent studies have used observation of similar bands as evidence for the migration of lithium ions to vacant octahedral sites.[16,18,21,23]

A possible explanation for discrepancies in the location of the lithium cations is provided by most recent investigations, which indicate that the sites to which lithium ions migrate is dependent on the degree and type of substitution exhibited by the montmorillonite.[18,23] More specifically, migration to octahedral sites is most favorable when the degree of substitution in the octahedral layer is high and that in the tetrahedral layer is low, whereas when the degree of substitution in the octahedral layer is low and that in the tetrahedral layer is high migration is almost exclusively to ditrigonal cavities. The same studies also show that only a small percentage of lithium ions that migrate to the ditrigonal cavities is irreversibly trapped, and so, fixation is highest when migration is predominantly to octahedral sites. Observations are therefore very sample-dependent.

Further insight into the effect of isomorphic substitution on lithium migration is afforded by classical Monte Carlo and molecular dynamics studies of hydrated lithium montmorillonite.[6,8] These simulations show that the location of lithium cations in the interlayer is greatly influenced by the isomorphic substitutions present in the tetrahedral and octahedral sheets. Two types of lithium solvation complex are observed as follows: (i) inner sphere complexes strongly bound to isomorphic substitution sites in the tetrahedral sheet and (ii) outer sphere complexes loosely associated with isomorphic substitutions sites in the octahedral sheet. Similar complexes have been reported for montmorillonite saturated with sodium,[5] potassium,[7] and cesium.[9] One could therefore postulate that the electrostatic interaction between lithium cations and tetrahedral aluminum is so great that it prevents further migration into vacant octahedral sites. Density functional studies of sodium montmorillonite have also shown the tendency of cations to lie close to sites of tetrahedral substitution.[25,26]

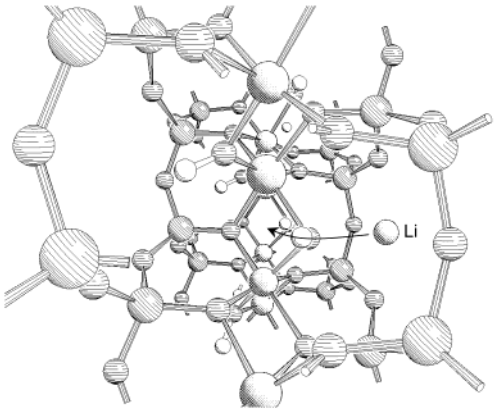

Figure 2. Migration of lithium from a ditrigonal cavity of the tetrahedral layer into a vacant octahedral site is inhibited by steric hindrance imposed by the hydroxyl group. The atoms types are distinguished as in Figure 1.

Despite the considerable literature on the migration of lithium cations from the interlayer into vacant octahedral sites, very few authors give any indication of how this may occur. Examination of the structure of montmorillonite shows that the steric hindrance imposed by hydroxyl groups inhibits migration of lithium cations from the ditrigonal cavities into vacant octahedral sites (Figure 2). The only authors to comment on the matter are Ebina et al. who suggest that thermal treatment leads to the vigorous movement of the hydroxyl hydrogens, which act as a kind of "crossing gate" making migration possible.[24]

Two insights that suggest possible ways in which lithium cations may overcome the steric hindrance of the hydroxyl groups are (i) that lithium ions react with hydroxyl groups to release protons[14,27,28] and (ii) that dehydroxylation of montmorillonite facilitates migration of cations into vacant octahedral sites.[29] Although dehydroxylation is normally considered to occur at higher temperatures (>500 °C),[28−34] some authors suggest that it may begin at temperatures as low as 200 °C.[35]

The purpose of the present study is to provide theoretical insight into the Hofmann−Klemen effect by employing density functional theory (DFT)-based methods to examine the phenomenon at the electronic structure level. Specifically, we investigate whether it is more favorable for the lithium cation to reside in the ditrigonal cavities of the tetrahedral layer or the vacant octahedral sites. We also examine possible mechanisms of migration of lithium cations from the ditrigonal cavity to a vacant octahedral site via deprotonation or dehydroxylation of

the clay. In addition, vibrational spectra are calculated and compared with experimental data.

The paper is organized as follows. In Section 2, we outline the model systems studied and the computational methods employed in our work. This is followed by a discussion of the results of the simulations in Section 3, beginning with the optimized structures, going on to the ab initio molecular dynamics calculations, and finishing with predicted vibrational spectra. Finally, in Section 4, we draw some conclusions from our work.

2. Simulation Details

In this section, we describe the model systems and methods used to perform geometry optimization and ab initio molecular dynamics and to calculate vibrational spectra. We also give some brief computational details concerning the calculations.

2.1. Model Systems. Because montmorillonite is naturally disordered in the planes of the clay layers, very little structural data are available in the common international X-ray crystallographic databases, where only the unit cell parameters are found.[36] It is therefore customary to create a montmorillonite model from the crystal structure of a closely related clay mineral. However, this has led to many studies of the wrong structural isomer.

In 2:1 layer type clay minerals, three distinct octahedral sites may be distinguished. These are designated cis or trans according to their position relative to the hydroxyl groups; two are cis, and one is trans. The existence of structural isomers arises with dioctahedral clays such as montmorillonite, since only two out of three octahedral sites are occupied. There is therefore the possibility of a structure in which one cis and one trans site are occupied, defined as cis vacant (cv) and one in which both cis cites are filled, known as trans vacant (tv).

Nearly all previous simulation studies of montmorillonite have looked at the tv isomer, since the models used were constructed from the crystal structure of a tv-related clay mineral. However, experimental evidence suggests that the naturally occurring material is of the cv form.[30−33] In classical molecular dynamics simulations, where interest is focused on events occurring in the interlayer, the choice of isomer can be expected to have little effect on computed behavior, but where the behavior of the hydroxyl groups is being studied, it may play a crucial role. Sainz-Diaz et al. looked at the cv and tv configurations of illites and smectites using transferable empirical interatomic potentials.[37] These authors found that although there was little difference in hydroxyl bond length for the two isomers, the angle that the hydroxyl groups made with the *ab* plane was slightly higher in the cv systems than in the tv systems.

A periodic model of cv pyrophyllite was therefore constructed from a tv pyrophyllite unit cell described elsewhere.[38] Pyrophyllite has identical aluminosilicate layers to montmorillonite but exhibits no isomorphic substitution in either the tetrahedral or the octahedral layer. This model was optimized as outlined in Section 2.2, with all atom and cell parameters allowed to vary.

From the optimized cv pyrophyllite model, a cv lithium montmorillonite model was formed, which exhibited a unit cell formula of $[LiMgAl_3(OH)_4(Si_4O_{10})_2]$, corresponding to one isomorphic substitution of aluminum by magnesium in the octahedral layer balanced by a lithium cation; two variations were fabricated, one with the cation located in a ditrigonal cavity of the tetrahedral layer and the other with it situated in a previously vacant octahedral site. These represented a montmorillonite with an unusually high degree of substitution in the octahedral layer. In the natural material, approximately one in eight aluminum atoms in the octahedral layer and one in 400 silicon atoms in the tetrahedral layer undergo substitution. However, to model such ratios exactly would have required a model so large as to make the calculations intractable.

To position the lithium cation in a ditrigonal cavity, the unit cell *c* parameter was fixed at 12 Å and a short (0.1 ps) molecular dynamics simulation was performed as outlined in Section 2.2. The cation, initially located at the center of the cell, equidistant between the clay layer and its periodic image, moved directly into a ditrigonal cavity during dynamics. For the second model, the lithium cation was placed in a vacant octahedral site manually. Each unit cell was assigned an initial *d* spacing of 9.60 Å before optimization, which corresponds to a unit cell *c* parameter of approximately 9.75 Å, based on previously reported swelling data for lithium montmorillonite.[5]

Partially deprotonated and dehydroxylated analogues were also created. Deprotonated models had one hydroxyl hydrogen removed and placed in the interlayer, while dehydroxylated models had one hydroxyl group and one hydroxyl hydrogen, i.e. H_2O, completely removed. In each case, the species were removed from the hydroxyl group(s) in closest proximity to the cation.

For comparison purposes, an additional model with the cation residing in the interlayer, hydrated by 10 water molecules, was generated from the optimized model with the lithium cation in a ditrigonal cavity. The model was given a *d* spacing of 17.00 Å, which corresponds to a unit cell *c* parameter of approximately 17.26 Å, again based on previously reported swelling data for lithium montmorillonite.[5]

2.2. Geometry Optimization and Molecular Dynamics. Geometry optimization and ab initio molecular dynamics calculations based on DFT were carried out using the CASTEP code,[39] which utilizes periodic boundary conditions, a plane wave basis set, and **k**-point sampling. Ultrasoft pseudopotentials were employed.[40] The energy cutoff for the plane wave expansion was 340 eV, and just one special **k**-point was allowed in the Brillouin zone, situated at (0.25,0.00,0.00). For all simulations, the form of the exchange−correlation functional used adhered to the generalized gradient approximation (GGA).[41,42]

Geometry optimization simulations were performed with all atom positions and cell parameters allowed to vary. To allow calculation of total energy differences between unit cells of different volume at a relatively low energy cutoff, a finite basis set correction was applied.[43] This corrects the total energies for errors due to the use of a finite **k**-point set in a finite cutoff energy calculation.

Molecular dynamics simulations were performed within the canonical (N,V,T) ensemble using a time step of 1.0 fs. For the model systems, with the lithium cation located in a ditrigonal cavity or an octahedral site, 3.0 ps was obtained at temperatures of 300 and 573 K, while for the larger hydrated model 2.0 ps was recorded at a temperature of 300 K.

2.3. Calculation of Power Spectra. Vibrational power spectra were calculated for all systems from the temporal Fourier transform of the velocity autocorrelation function (VACF) determined from the molecular dynamics simulations at 300 K. In each case, the first 0.5 ps of each simulation was allowed for equilibration and the VACFs were calculated over the remaining time. The VACFs were calculated up to the maximum value, with the time origins at every time step, but truncated at 0.4 ps prior to Fourier transformation, giving a resolution of 41.67 cm^{-1} (or $\pm$1.2 THz).

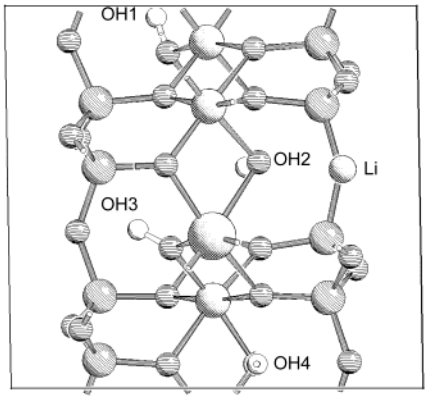

Figure 3. Optimized lithium montmorillonite unit cell with cation situated in a ditrigonal cavity of the tetrahedral layer. Three-dimensional periodic boundary conditions are applied at the edges of the cell, as indicated by the solid lines. The atom types are distinguished as in Figure 1.

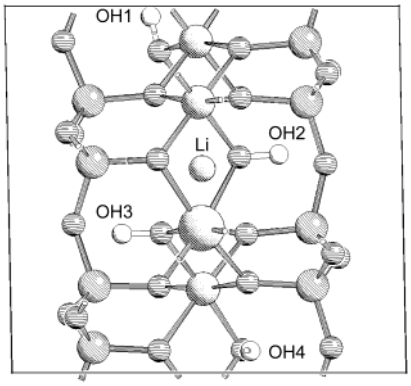

Figure 4. Optimized lithium montmorillonite unit cell with cation situated in a previously vacant octahedral site. Three-dimensional periodic boundary conditions are applied at the edges of the cell, as indicated by the solid lines. The atom types are distinguished as in Figure 1.

2.4. Computational Details. The computational cost of ab initio molecular dynamics requires the use of parallel machines. The majority of calculations were run on a Silicon Graphics Onyx2 mounted with 16 400 MHz MIPS R12000 processors and eight GB RAM. Some calculations were also performed on an 816-processor CRAY T3E-1200E. The CASTEP code scales well up to 16 processors for our systems.

3. Results and Discussion

In this section, we discuss the results of our simulations. We begin by giving details of the optimized periodic lithium montmorillonite structures. This is followed by an account of observations made from the ab initio molecular dynamics simulations. Finally, we analyze the calculated power spectra.

3.1. Geometry Optimization. Figures 3 and 4 illustrate the optimized cv montmorillonite models with the lithium cation located in a ditrigonal cavity of the tetrahedral layer and a previously vacant octahedral site, respectively. These will subsequently be referred to as the cv-tetra and cv-octa models, respectively.

Deprotonation and dehydroxylation were not observed during the optimization of the models. However, this is not surprising since these were 0 K calculations, where thermal energy is not considered. The unit cell parameters of the optimized models are listed in Table 1. Those reported from crystallographic data for montmorillonite are also listed for comparison;[36] although no information was available on the exact nature of the sample, it is presumed to be a natural, dehydrated clay. The calculated unit cell parameters show little deviation from those reported from experiment. The only interesting result is the larger *a* and *b* parameters exhibited by the cv-octa model, required to accommodate the lithium cation in the octahedral layer.

TABLE 1: Unit Cell Parameters of Optimized Lithium Montmorillonite Models

model[a]	*a*	*b*	*c*	α	*β*	*γ*
experiment[31]	5.18	8.96	9.97	90.0	99.9	90.0
cv-tetra	5.19	9.00	9.77	89.0	97.3	90.3
cv-octa	5.21	9.02	9.77	88.6	97.5	90.0

[a] Lengths are given in Å, and angles are given in deg.

TABLE 2: O−H Bond Lengths of Optimized Lithium Montmorillonite Models (Å)

model[a]	OH1	OH2	OH3	OH4
cv-tetra	0.973	0.981	0.966	0.974
cv-octa	0.974	0.972	0.971	0.974

[a] O−H bond labels refer to Figures 3 and 4.

TABLE 3: Angles between *ab* Plane and O−H Bonds of Optimized Lithium Montmorillonite Models (deg)

model[a]	OH1	OH2	OH3	OH4
cv-tetra	−15.9	−18.0	−51.9	+3.50
cv-octa	−12.0	+82.7	−89.5	+11.5

[a] O−H bond labels refer to Figures 3 and 4.

The total energy of the optimized cv-octa model was 87.9 kJ mol^{-1} lower than that of the cv-tetra model, which indicates that it is energetically more favorable for the lithium cation to reside in an octahedral site than within a ditrigonal cavity of the tetrahedral layer. This is probably due to the closer proximity of the lithium cation to the negative charge site when in the octahedral layer, increasing favorable Coulombic interactions. The lithium−magnesium distances are 3.545 and 2.973 Å for the optimized cv-tetra and cv-octa models, respectively. Ebina et al. performed density functional-based calculations on cluster models of lithium montmorillonite and reported lithium−magnesium distances of 3.535 and 2.610 Å, when the cation was located in the ditrigonal cavity of the tetrahedral layer and a previously vacant octahedral site, respectively.[24] The reason for the comparatively shorter lithium−magnesium distance calculated by these authors, in the case where the lithium cation is located in a previously vacant octahedral site, is likely due to their use of a local geometry optimization method.

The idea that increased proximity of lithium cations to isomorphic substitutions in the octahedral layer increases stability corroborates experimental observations that fixation in octahedral sites is greatest when the degree of substitution in the octahedral layer is high.[18,23]

The bond lengths of the hydroxyls present in our optimized models are listed in Table 2. The hydroxyl bond lengths are all very similar to each other. The longest hydroxyl bond is that whose oxygen is coordinated to a lithium ion located in a ditrigonal cavity, i.e., OH(2) of the cv-tetra model.

The angle that each hydroxyl group present in the optimized models makes with the *ab* plane is listed in Table 3. The cv-octa model exhibits two hydroxyls making an angle of approximately 90° to the *ab* plane and two lying parallel to the plane. Such large angles are not observed for the cv-tetra model. These results confirm the simple calculations of Calvet and Prost who, as we discussed earlier, reported that the filling of vacant octahedral sites in montmorillonite results in stability only if

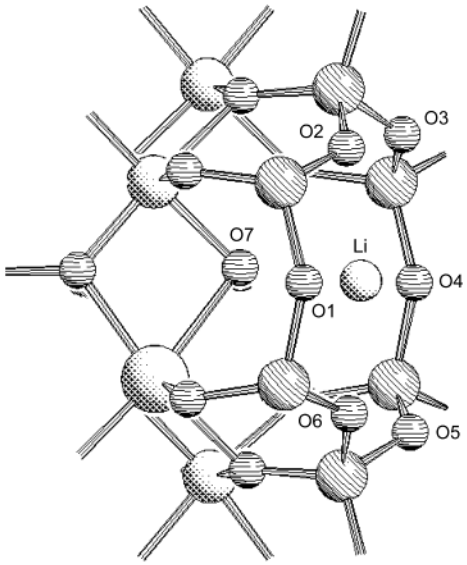

Figure 5. Fragment showing the coordination of lithium by oxygen when situated in a ditrigonal cavity of the tetrahedral layer. The atom types are distinguished as in Figure 1.

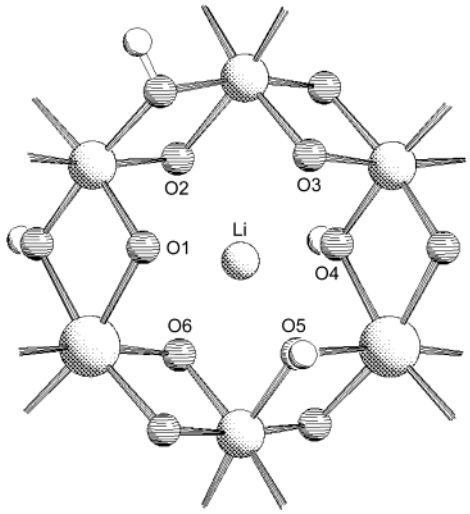

Figure 6. Fragment showing the coordination of lithium by oxygen when situated in a previously vacant octahedral site. The atom types are distinguished as in Figure 1.

TABLE 4: Li−O Distances of Optimized Lithium Montmorillonite Models (Å)

model[a]	Li−O1	Li−O2	Li−O3	Li−O4	Li−O5	Li−O6	Li−O7
cv-tetra	2.538	2.307	2.724	2.654	2.795	2.298	1.976
cv-octa	2.198	2.167	2.383	2.070	2.042	2.128	

[a] Li−O labels refer to Figures 5 and 6.

neighboring structural hydroxyl groups reorientate perpendicular to the *ab* plane—the suggested origin of the dichroic nature of hydroxyl stretching bands observed in the infrared spectrum of heat-treated lithium montmorillonite being a corollary of this.[19]

Figures 5 and 6 show the coordination of lithium by oxygen in the cv-tetra and cv-octa models, respectively. Associated Li−O distances are given in Table 4. In the cv-tetra model, the lithium cation is essentially three coordinate, bonding to O2 and O6 of the hexagonal ring and O7, the hydroxyl oxygen at the bottom of the ditrigonal cavity. In the case of the cv-octa model, coordination is, as expected, octahedral type. The average Li−O bond length is 2.165 Å. This compares reasonably well with 2.130 Å, the average Li−O bond length for a $[Li(H_2O)_6]^+$ cluster, calculated using second-order Møller Plesset (MP2) perturbation theory and a 6-31+G(d) basis set.[44] In both instances, the shortest Li−O bonds are those made between the lithium cation and the hydroxyl oxygen.

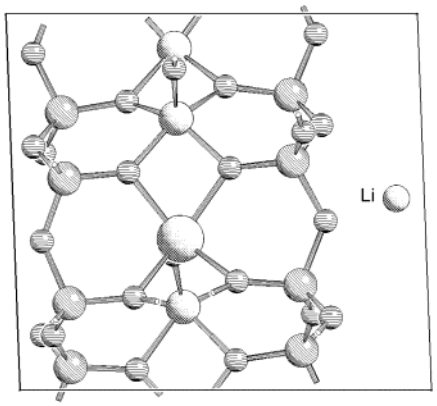

Figure 7. tv dehydroxylated structure formed upon optimization of fully dehydroxylated cv lithium montmorillonite model. During rearrangement, the cation moves from the ditrigonal cavity of the tetrahedral layer into the interlayer. Three-dimensional periodic boundary conditions are applied at the edges of the cell, as indicated by the solid lines. The atom types are distinguished as in Figure 1.

These results all indicate that migration of lithium ions into vacant octahedral sites does indeed occur, albeit without providing a pathway. The total energy of the optimized deprotonated cv-octa model was 80.1 kJ mol^{-1} lower than that of the cv-tetra model. This trend is seen again with the total energy of the optimized dehydroxylated cv-octa model being 32.8 kJ mol^{-1} lower than that of the cv-tetra model.

The geometry of the deprotonated models remained largely unperturbed upon optimization. The energy-minimized structures for the most part resembled their parent models shown in Figures 3 and 4, simply with a proton removed. The most notable change occurred in the model where the lithium ion was located in a ditrigonal cavity, where a decrease was observed in the lithium−oxygen distance, for that oxygen from which the proton was removed. The deprotonated cv-tetra model exhibited a value of 1.786 Å, as compared to 1.976 Å for the corresponding parent model. The lithium ion associated strongly with the residual oxygen.

Muller et al. suggest that upon dehydroxylation, cv and tv montmorillonite form the same tv layer structure where the residual oxygen atoms locate themselves within the plane of the octahedral aluminum ions, which provide homogeneous local charge compensation.[31] The formation of the tv dehydroxylated structure from cv montmorillonite is said by these authors to occur in two stages: initially, dehydroxylation occurs and the residual oxygen atoms relocate themselves within the octahedral plane, after which the octahedral aluminum cations migrate to form a tv state, which brings about the stabilization of the arrangement.

In the case of our geometry-optimized cv-tetra model, the lithium associated itself with the residual oxygen, which showed no movement into the octahedral layer. Similarly, no movement of the residual oxygen into the octahedral plane was observed for the cv-octa model. However, further investigation showed that when the cv-tetra model was fully dehydroxylated before energy minimization, it did indeed rearrange to form a tv-dehydroxylated structure, as shown in Figure 7. The movement of the residual oxygen atoms into the plane of the octahedral aluminum ions occured concurrently with and was dependent on the migration of the octahedral ions into the tv state.

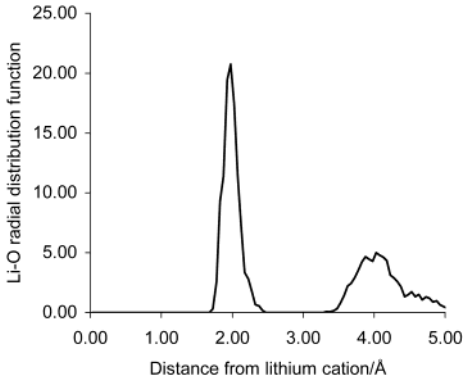

Figure 8. Li−O radial distribution function for the interlayer water of the hydrated lithium montmorillonite model, evaluated over the final 2 ps of ab initio molecular dynamics at 300 K.

It is interesting to note that the movement of the residual oxygen atoms within the plane of the octahedral ions yields a much less sterically hindered pathway for lithium migration to vacant sites in the octahedral layer. However, no migration was observed during optimization of the dehydroxylated models. In fact, the opposite was observed: the lithium cation moved out of the ditrigonal cavity and into the interlayer. This is probably because the negative charge of the residual oxygen is shielded between the octahedral ions so that the driving force for the lithium ion to enter the ditrigonal cavity is removed. These observations indicate that dehydroxylation inhibits rather than aids migration of the cations into the clay lattice.

Although lithium migration was not observed during the geometry optimization of the cv-tetra model, we again note that this is a 0 K calculation, where thermal energy is not considered. To be able to take into account the thermal energy available when the lithium montmorillonite is heated to 300 °C, molecular dynamics was performed, as described in the following subsection.

3.2. Ab Initio Molecular Dynamics. Molecular dynamics simulations were performed for the cv-tetra and cv-octa models. The simulations showed that both models were stable toward deprotonation and dehydroxylation at 300 and 573 K, at least on the time scale of the simulations. Migration of the cation into a vacant octahedral site was not observed for the cv-tetra model at either temperature—this is likely due to the short simulation time. The constraint that cell parameters must remain fixed during the molecular dynamics may also have restricted the movement of the atoms. Indeed, our geometry optimizations show that the unit cell *a* and *b* parameters must increase in order to accommodate the lithium cation in the octahedral layer.

Figure 1 shows a snapshot from the molecular dynamics simulation of the hydrated lithium montmorillonite model at 300 K. The Li−O radial distribution function for the interlayer water is shown in Figure 8 and is in good agreement with that calculated by Chang et al. from classical molecular dynamics studies,[6] exhibiting a main peak at 2.00 Å. The lithium counterion was observed to be predominantly hydrated by four water molecules, with short intervals when this reduced to three. This is in good accord with classical simulations of Sposito et al.[8] The lithium ion did not, however, venture into a ditrigonal cavity at any point during the simulation or even approach close, probably due to its hydration sphere.

The most useful observations emanating from these simulations concerned the orientation of the hydroxyl groups in the cv-octa model. The geometry optimization calculations had already shown that migration of the lithium cation into a previously vacant octahedral site causes orientation of neighboring hydroxyl groups approximately 90° to the *ab* plane. The molecular dynamics simulations showed that even at finite temperature the same hydroxyl groups fluctuated little from this angle.

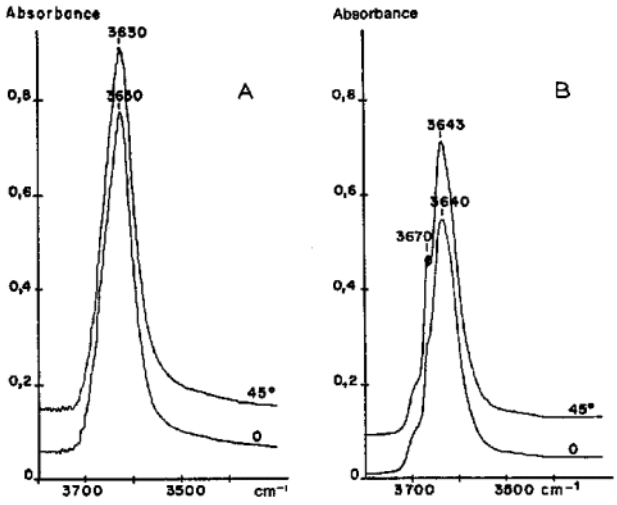

Figure 9. Stretching vibrations of structural hydroxyl groups of lithium montmorillonite; (A) unheated; (B) heated at 220 °C for 24 h. Dichroic properties are observed by tilting the film in the incident beam from 0 to 45°. Reproduced from Calvet and Prost[19] with permission.

3.3. Power Spectra. Vibrational spectra have previously been calculated for clay minerals.[45−51] When employing ab initio techniques to calculate vibrational spectra, it has been usual to employ a second derivative based-method and study cluster models.[45,46] The problem with cluster models is that they are unable to take into account the existence of hydrogen bonding between hydroxyl hydrogens and apical oxygen atoms of the tetrahedral sheet, which causes calculated hydroxyl stretching frequencies to be lower than expected.[46] More recent investigations have therefore taken a different route and calculated power spectra from the Fourier transformation of the VACF obtained from the trajectories of relatively short (1 ps) molecular dynamics simulations of a periodic model.[48−50] This technique is discussed in detail by Kleinhesselink and Wolfsberg who recommend the use of long trajectories coupled with truncation of the VACF prior to its Fourier transform in such a way that the tail of the VACF is disregarded.[52]

Truncation is employed to smooth the power spectra by excluding statistical noise in the tail of the VACF. It has been shown to have little effect on the position of band maxima in power spectra, although it has a noticeable affect on bandwidth.[52] In our work, the calculated VACFs were truncated at 0.4 ps before Fourier transformation—this was the approximate value at which all of the VACFs had decayed to a minimum level. If truncation was omitted, the spectra showed bands with multiplet type structure.

More preferable to truncation would have been ensemble averaging by computing multiple trajectories; however, this is not currently tractable due to the computational expense involved. Experimentation with simulation time showed that if a VACF was calculated using just 1ps of a trajectory (ignoring the first 0.5 ps) and then using 2 ps, differences of up to 30 cm^{-1} were observed in band maxima, indicating the necessity of long trajectories for quantitatively reliable results, again inhibited by computational cost.

Before examining the calculated spectra, it is useful to consider the experimentally observed changes in the infrared spectrum of lithium montmorillonite upon thermal treatment. Figure 9 shows experimental infrared spectra recorded by Calvet

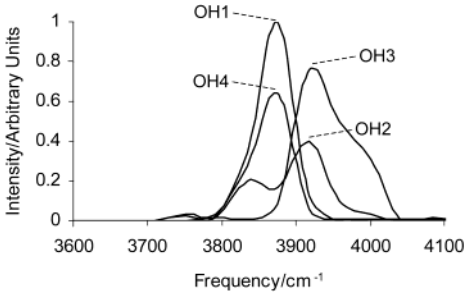

Figure 10. Calculated power spectrum for O−H stretching region when the lithium cation is hydrated in the interlayer. Hydroxyl labels refer to Figure 1.

and Prost.[19] Before thermal treatment, the O−H stretching region of the infrared spectrum exhibits just a single, nondichroic band at 3630 cm^{-1}, but after it is heated, several new bands are observed: a dichroic band at 3670 cm^{-1} assigned to an AlMgLiOH configuration; a second dichroic band at slightly lower frequency attributed to an AlAlLiOH arrangement; and a shoulder at 3700 cm^{-1} due to MgMgLiOH. (Here, the three metal ions indicate the trioctahedral arrangement to which a structural hydroxyl group is bonded.) Similar observations have been reported by many other authors.[16,18,21,23] We also note that in montmorillonites that exhibit an unusually high degree of substitution in the tetrahedral layer there is no observed change.[23]

The power spectrum calculated for the cv-hydrated model is shown in Figure 10. It shows a group of OH stretching bands centered around 3880 cm^{-1}. Hydroxyls OH2 and OH3 still show some multiplet structure, probably an artifact of the short trajectory. One would not expect the calculated spectrum to exhibit an identical profile to that produced by experiment. Experimental vibrational spectra of montmorillonite show the sum of the vibrational frequencies of a vast number of hydroxyl groups, in a large number of different local environments, whereas the calculated power spectrum displays the individual frequencies of four such groups, in a few selected coordination states. Even where an experimental vibrational frequency may be assigned explicitly, a calculated frequency is not normally expected to be in good quantitative agreement. For ab initio second derivatives methods, it is customary to multiply frequencies by a scaling factor, to improve agreement with experimental results.[53−56] No such scaling factor exists for frequencies calculated from the Fourier transformation of autocorrelation functions.

However, the advantage of calculated spectra is that one is able to observe the vibrational frequency of an individual hydroxyl group and investigate the effect of varying its local environment. As such, this spectrum will be used as a reference from which relative shifts due to the migration of the lithium cation can be calculated.

The power spectrum calculated for the cv-tetra model is shown in Figure 11. Calculated stretching frequencies for OH1, OH2, OH3, and OH4 are approximately 3875, 3710, 3960, and 3830 cm^{-1}, respectively. These values correlate well with the corresponding hydroxyl bond lengths of the optimized cv-tetra model listed in Table 2. Indeed, previous theoretical studies of clay minerals have shown an approximate linear relationship between calculated hydroxyl stretching frequency and bond length.[48−50] One can see that the frequencies of OH1 and OH4 lie in the same range as the OH stretching band observed for the cv-hydrated model, while that of OH2, which interacts directly with the lithium cation, is much lower and that of OH3 is much higher. Although the band due to OH3 could possibly be assigned to the shoulder at higher frequencies, that associated

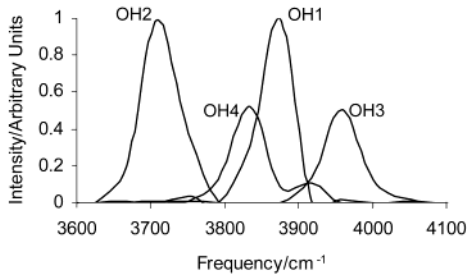

Figure 11. Calculated power spectrum for the O−H stretching region when the lithium cation is located in the ditrigonal cavity of the tetrahedral layer. Hydroxyl labels refer to Figure 3.

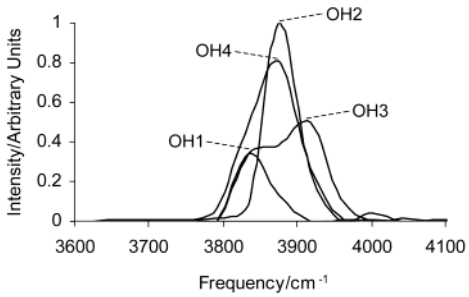

Figure 12. Calculated power spectrum for the O−H stretching region when the lithium cation is located in a previously vacant octahedral site. Hydroxyl labels refer to Figure 4.

with OH2 at lower frequencies is not observed experimentally for any type of montmorillonite. The disagreement with spectra for montmorillonites where tetrahedral charge is low is not surprising since we expect the cations to be in octahedral sites. However, it is interesting that the spectrum is also in disagreement with those reported for montmorillonites with a high degree of substitution in the tetrahedral layer, where the lithium cations are thought to be present in the ditrigonal cavities.[23] A possible explanation is that in these types of clay the lithium cations associate so strongly with the tetrahedral aluminum that they are unable to penetrate deep enough into the ditrigonal cavities to interfere with structural hydroxyl groups. Hence, there is little change observed in the spectrum upon heating.

The power spectrum calculated for the cv-octa model is shown in Figure 12. Stretching frequencies for OH1, OH2, OH3, and OH4 are approximately 3840, 3870, 3875, and (3850 and 3910 cm^{-1}), respectively. As above, these values correlate well with the corresponding hydroxyl bond lengths of the optimized cv-octa model listed in Table 2. Together, they form a band centered around 3880 cm^{-1}, in the same position as that observed for the hydrated model. There is no indication of a new band or shoulder at higher frequency; indeed, as compared with the spectrum of the hydrated clay, the bands associated with OH2 and OH3 occur at lower frequencies. However, overall, the calculated spectrum for the cv-octa model is in much better agreement with that observed experimentally for thermally treated lithium montmorillonite than that of the cv-tetra model. This implies that migration is normally to vacant octahedral sites in clays with a low degree of tetrahedral substitution.

We are unable to conclusively confirm experimental assignments. The short length of the dynamics trajectories means that the accuracy of the calculated spectra is not high enough to be able to resolve the smaller band shifts observed experimentally.

4. Conclusions

We conclude that migration of lithium cations into previously vacant octahedral sites of montmorillonite causes orientation

of structural hydroxyl groups perpendicular to the *ab* plane. It is energetically preferable for lithium cations to reside in previously vacant octahedral sites rather than in ditrigonal cavities, due to the closer proximity of the lithium cations to negative charge sites in the octahedral layer increasing favorable Coulombic interactions. Dehydroxylation inhibits migration of lithium cations to octahedral sites. The large shifts observed in the calculated power spectrum for the cv-tetra model, but not in experimental spectra, suggest that lithium cations do not migrate to ditrigonal cavities when no tetrahedral aluminum is present.

Acknowledgment. We are grateful to HEFCE (U.K.) for funding the purchase of our Silicon Graphics Onyx2 machine under the JREI scheme. We also acknowledge EPSRC for providing access to the Cray T3E-1200E maintained by CSAR under Grant No. GR/R30907. The Ph.D. studentship of S.S. is funded by Queen Mary, University of London, and W. R. Grace & Co.

References and Notes

(1) Calvet, R. *Ann. Agron.* **1973**, *24*, 77.
(2) Fu, M. H.; Zhang, Z. Z.; Low, P. F. *Clays Clay Miner.* **1990**, *38*, 485.
(3) Delville, A.; Laszlo, P. *Langmuir* **1990**, *6*, 1289.
(4) Delville, A. *Langmuir* **1991**, *7*, 547.
(5) Boek, E. S.; Coveney, P. V.; Skipper, N. T. *J. Am. Chem. Soc.* **1995**, *117*, 12608.
(6) Chang, F.-R. C.; Skipper, N. T.; Sposito, G. *Langmuir* **1997**, *13*, 2074.
(7) Chang, F.-R. C.; Skipper, N. T.; Sposito, G. *Langmuir* **1998**, *14*, 1201.
(8) Greathouse, J.; Sposito, G. *J. Phys. Chem. B* **1998**, *102*, 2406.
(9) Smith, D. E. *Langmuir* **1998**, *14*, 5959.
(10) Park, S.-H.; Sposito, G. *J. Phys. Chem. B* **2000**, *104*, 4642.
(11) Bains, A. S.; Boek, E. S.; Coveney, P. V.; Williams, S. J.; Akbar, M. V. *Mol. Simul.* **2001**, *26*, 101.
(12) Hofmann, U.; Klemen, R. *Z. Anorg. Allg. Chem.* **1950**, *262*, 95.
(13) Tettenhorst, R. *Am. Miner.* **1962**, *47*, 769.
(14) Alvero, R.; Alba, M. D.; Castro, M. A.; Trillo, J. M. *J. Phys. Chem.* **1994**, *98*, 7848.
(15) Theng, B. K. G.; Hayashi, S.; Soma, M.; Seyama, H. *Clays Clay Miner.* **1997**, *45*, 718.
(16) Srasra, E.; Bergaya, F.; Fripiat, J. J. *Clays Clay Miner.* **1994**, *42*, 237.
(17) Karakassides, M. A.; Gournis, D.; Petridis, D. *Clay Miner.* **1999**, *34*, 429.
(18) Hrobáriková, J.; Madejová, J.; Komadel, P. *J. Mater. Chem.* **2001**, *11*, 1452.
(19) Calvet, R.; Prost, R. *Clays Clay Miner.* **1971**, *19*, 175.
(20) Sposito, G.; Prost, R.; Gaultier, J.-P. *Clays Clay Miner.* **1983**, *31*, 9.
(21) Madejová, J.; Arvaiová, B.; Komadel, P. *Spectrochim. Acta A* **1999**, *55*, 2467.
(22) Karakassides, M. A.; Madejová, J.; Arvaiová, B.; Bourlinos, A.; Petridis, D.; Komadel, P. *J. Mater. Chem.* **1999**, *9*, 1553.
(23) Madejová, J.; Bujdák, J.; Petit, S.; Komadel, P. *Clay Miner.* **2000**, *35*, 739.
(24) Ebina, T.; Iwasaki, T.; Chatterjee, A. *Clay Sci.* **1999**, *10*, 569.
(25) Chatterjee, A.; Iwasaki, T.; Ebina, T.; Miyamoto, A. *Comput. Mater. Sci.* **1999**, *14*, 119.
(26) Chatterjee, A.; Iwasaki, T.; Ebina, T. *J. Phys. Chem. A* **2000**, *104*, 8216.
(27) Heller-Kallai, L. *Appl. Clay Sci.* **2001**, *20*, 27.
(28) Bujdák, J.; Slosiariková, H. *J. Therm. Anal.* **1994**, *41*, 825.
(29) He, H. P.; Guo, J. G.; Xie, X. D.; Peng, J. L. *Environ. Int.* **2001**, *26*, 347.
(30) Drits, V. A.; Besson, G.; Muller, F. *Clays Clay Miner.* **1995**, *43*, 718.
(31) Muller, F.; Drits, V.; Plançon, A.; Robert, J.-L. *Clays Clay Miner.* **2000**, *48*, 572.
(32) Emmerich, K.; Kahr, G. *Appl. Clay Sci.* **2001**, *20*, 119.
(33) Emmerich, K.; Plötze, M.; Kahr, G. *Appl. Clay Sci.* **2001**, *19*, 143.
(34) Bray, H. J.; Redfern, S. A. T. *Mineral. Mag.* **2000**, *64*, 337.
(35) Bala, P.; Samantaray, B. K.; Srivastava, S. K. *Bull. Mater. Sci.* **2000**, *23*, 61.
(36) Wyckoff, R. W. G. *Crystal Structures*; John Wiley and Sons: Chichester, 1968; Vol. 4, p 372.
(37) Sainz-Diaz, C. I.; Hernández-Laguna, A.; Dove, M. T. *Phys. Chem. Miner.* **2001**, *28*, 322.
(38) Stackhouse, S.; Coveney, P. V.; Sandré, E. *J. Am. Chem. Soc.* **2001**, *47*, 11764.
(39) Payne, M. C.; Teter, M. P.; Allan, D. C.; Arias, T. A.; Joannopoulos, J. D. *Rev. Mod. Phys.* **1992**, *64*, 1045.
(40) Vanderbilt, D. *Phys. Rev. B* **1990**, *41*, 7892.
(41) Perdew, J. P.; Chevary, J. A.; Vosko, S. H.; Jackson, K. A.; Perderson, M. R.; Singh, D. J.; Fiolhais, C. *Phys. Rev. B* **1992**, *46*, 6671.
(42) White, J. A.; Bird, D. M. *Phys. Rev. B* **1994**, *50*, 4954.
(43) Francis, G. P.; Payne, M. C. *J. Phys.: Condens. Mater.* **1990**, *2*, 4395.
(44) Yamaji, K.; Makita, Y.; Watanabe, H.; Sonoda, A.; Kanoh, H.; Hirotsu, T.; Ooi, K. *J. Phys. Chem. A* **2001**, *105*, 602.
(45) Chatterjee, A.; Iwasaki, T.; Ebina, T.; Hayashi, H. *J. Mol. Graph.* **1996**, *14*, 302.
(46) Sainz-Diaz, C. I.; Timon, V.; Botella, V.; Hernandez-Laguna, A. *Am. Mineral.* **2000**, *85*, 1038.
(47) Bougeard, D.; Smirnov, K. S.; Geidel, E. *J. Phys. Chem. B* **2000**, *104*, 9210.
(48) Benco, L.; Tunega, D.; Hafner, J.; Lischka, H. *Am. Mineral.* **2001**, *86*, 1057.
(49) Benco, L.; Tunega, D.; Hafner, J.; Lischka, H. *Chem. Phys. Lett.* **2001**, *333*, 479.
(50) Benco, L.; Tunega, D.; Hafner, J.; Lischka, H. *J. Phys. Chem. B* **2001**, *105*, 10812.
(51) Balan, E.; Saitta, A. M.; Mauri, F.; Calas, G. *Am. Mineral.* **2001**, *86*, 1321.
(52) Kleinhesselink, D.; Wolfsberg, M. *Surf. Sci.* **1992**, *262*, 189.
(53) Rauhut, G.; Pulay, P. *J. Phys. Chem.* **1995**, *99*, 3093.
(54) El-Azhary, A. A.; Suter, H. U. *J. Phys. Chem.* **1996**, *100*, 15056.
(55) Scott, A. P.; Radom, L. *J. Phys. Chem.* **1996**, *100*, 16502.
(56) Halls, M. D.; Velkovski, J.; Schlegel, H. B. *Theor. Chem. Acc.* **2001**, *105*, 413.